ELSEVIER

International Journal of Heat and Fluid Flow 20 (1999) 507–512

International Journal of HEAT AND FLUID FLOW

www.elsevier.com/locate/ijhff

# Surface wave transition before breakup on a laminar liquid jet

M. Arai *, K. Amagai

*Department of Mechanical System Engineering, Gunma University 1-5-1, Tenjin-cho, Kiryu, Gunma 376-8515, Japan*

**Abstract**

Problems of liquid jet breakup are very fundamental in the fluid-dynamics and application fields of atomization. Instability theories of the surface wave were usually used to describe the breakup phenomena. In these theories, it was assumed that the surface wave was a regular sinusoidal wave. However, irregular surface waves were frequently observed even though a liquid jet was laminar. In this paper, the surface wave structure on a vertically injected laminar liquid jet was experimentally investigated. The amplitude of the surface wave was detected by a photo-sensor system and its frequency spectrum was derived by an FFT analyzer. In the spectrum, there were many discrete peaks which were not in harmonic relation with each other. Further, a broad band spectrum appeared near the breakup point. These results indicated that the surface wave consisted of several waves with various modes. The breakup phenomena included the irregular motions even in a laminar liquid jet. Cross-correlation between two waves at different positions of the liquid column was derived. Since the similarity between two waves was evaluated by the cross-correlation function, the surface wave transition along the flow direction could be obtained. When the surface wave grew up to the large amplitude wave near the breakup point, it changed rapidly from regular to irregular wave. 

*Keywords:* Liquid jet; Surface wave; Liquid jet breakup; Frequency analysis of waves

**Notation**

| | |
|---|---|
| $d$ | liquid column diameter |
| $D$ | nozzle diameter |
| $E$ | output voltage of sensor signal |
| $f$ | frequency |
| $L_b$ | breakup length |
| $P(f)$ | power spectrum |
| $R(\Delta t)$ | cross-correlation |
| $v$ | liquid velocity |
| $V$ | injection velocity |
| $w$ | wave velocity |
| $z$ | distance from nozzle exit |
| $\Delta t$ | time delay |
| $\lambda$ | wavelength |
| *Superscript* | |
| * | dimensionless variable |
| *Subscript* | |
| 1 | sensor-1 |
| 2 | sensor-2 |

## 1. Introduction

A large number of studies of the breakup phenomena for the liquid jets injected from a round nozzle have been made by many researchers (for example, Tanasawa and Toyoda, 1955; Bogy, 1975). The temporal and spatial instability theories have been applied to predict the onset of surface waves and to describe the breakup phenomena of the liquid column (for example, Tomotika, 1935; Rayleigh, 1945; Keller et al., 1973). In the linear instability theories, it was assumed that the amplitude of the initial surface wave was very small compared with the liquid column diameter. These theories had been applied on the laminar liquid jet which had a smooth surface and was observed in the case of low injection velocity. Non-linear instability theories had been applied to describe the behavior of large amplitude waves on the liquid surface (Chaudhary and Redekopp, 1980). Results of these theories were compared with the experiments, and it was confirmed that the theoretical results agreed well with the experimental data (for example Donnely and Glaberson, 1966). In these theoretical works, the liquid column diameter was modeled to be constant. However, in the case of a vertically injected laminar jet when the injection velocity was comparatively low, the liquid column diameter changed vertically by the gravity effect. It seemed that the surface wave structure and breakup phenomena were influenced by the change of liquid column diameter. Our previous experiment showed that the naturally generated surface wave on the liquid column had a very complex structure (Amagai and Arai, 1997). This situation was much different from the modeling in the instability theory. Therefore, we need more

* Corresponding author. E-mail: arai@me.gunma-u.ac.jp

0142-727X/99/$ – see front matter 
PII: S0142-727X(99)00039-9

detailed information about the surface wave structure on a laminar liquid jet for understanding of the liquid jet breakup phenomena.

In this paper, we described the surface wave structure by employing the frequency analysis. Wavelength of the surface wave was derived from its frequency spectrum. It was compared with that of the instability wave predicted by the Rayleigh's instability theory (Rayleigh, 1945). Moreover, the cross-correlation analysis was carried out to investigate the spatial structure of the surface wave on the liquid column. The surface waves at two different positions on the liquid column were measured and the cross-correlation was derived by an FFT analyzer. From these data, the similarity of the wave motions between two points was evaluated. It provided new knowledge about the wave structure and breakup phenomena of the laminar liquid jet.

## 2. Experimental apparatus

A schematic representation of the experimental apparatus used is shown in Fig. 1. Tap water was used as a test liquid and was supplied into a round nozzle from an air pressurized tank. Valves, a pressure gauge and a flow meter were located in the water feed line to provide the desired injection flow rate. Here, the Reynolds number in a flow condition was defined by a nozzle diameter, dynamic viscosity of water and a mean injection velocity. The injection of the water was vertically downward. A stroboscope and a 35 mm camera were used to observe the wave formation on the liquid column.

Photo-sensor systems are illustrated in Fig. 2. Two sensor systems could traverse on the various vertical positions $z$ (distance from nozzle exit was denoted as $z$). This system consisted of a laser-diode of sheeted light and a photo-detector. The frequency response of this detector was enough to analyze the wave motion with frequency less than 10 kHz. The thickness of the laser sheet was 1.2 mm. The light absorption corresponding to the diameter of the liquid column can be measured by this sensor system. Output of the sensor was processed by a fast Fourier transform (FFT) analyzer to obtain the frequency spectrum and cross-correlation.

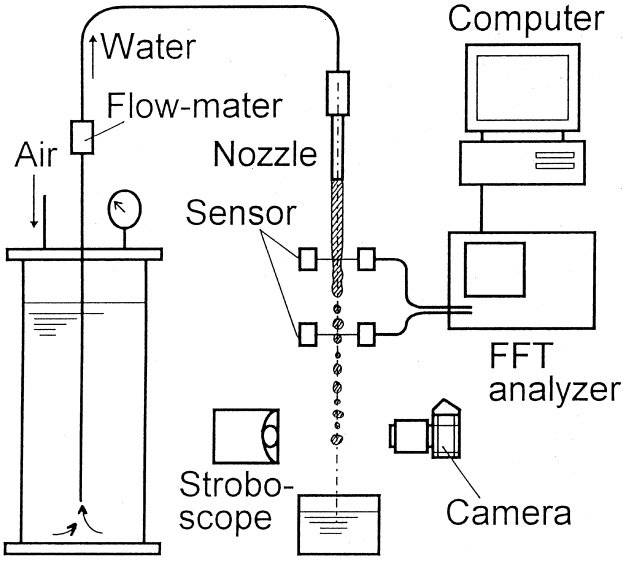


Fig. 1. Experimental apparatus.

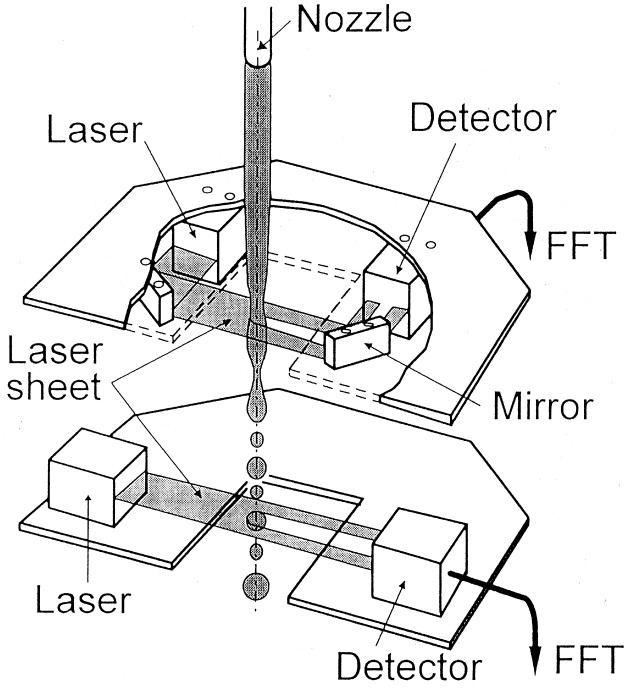


Fig. 2. Photo-sensor systems.

A sequential variation of axisymmetrical wave motions or liquid diameter changes detected by the photo-sensor are described as:

$$E = E(t), \tag{1}$$

where $E$ and $t$ mean the output voltage of the detector and time, respectively. The power spectrum $P(f)$ and cross-correlation $R(\Delta t, z_1, z_2)$ were calculated by:

$$P(f) = \left| \int_0^\infty E(t) \exp(-\mathrm{i}2\pi f t)\, \mathrm{d}t \right|, \tag{2}$$

$$R(\Delta t, z_1, z_2) = \frac{\langle E_1(t, z_1) E_2(t - \Delta t, z + z_2) \rangle}{\left\langle \sqrt{E_1^2(t, z_1)} \sqrt{E_2^2(t, z_2)} \right\rangle}, \tag{3}$$

where $f$ means frequency and i is the $\sqrt{-1}$, $E_1(t)$ and $E_2(t)$ the output voltages of detectors, $\Delta t$ a time delay, $z_1$ and $z_2$ the positions of sensors, and $\langle\ \rangle$ means the time average.

## 3. Results and discussions

### 3.1. Measurement of wave velocity

First of all, the wave velocity was measured by using the photo-sensor systems. The photo-sensor could detect an amplitude of the axisymmetrical surface wave which passed to the sensor at position $z$. Here by using the photo-observation, we confirmed that the surface waves on the liquid column were almost axisymmetric. The relation between frequency $f(z)$, wavelength $\lambda(z)$ and wave velocity $w(z)$ was described as:

$$f(z) = \frac{w(z)}{\lambda(z)}. \tag{4}$$

A cross-correlation method was used to measure the wave velocity. Two photo-sensors were fixed with a gap of $\Delta z = 10$ mm. Cross-correlation function was derived from the signals of two detectors. Time delay $\Delta t$ of the surface wave passing

between two light sheets was derived from the maximum peak position in the cross-correlation. Then, wave velocity $w$ was calculated by the following relation:

$$w = \frac{\Delta z}{\Delta t}. \tag{5}$$

Resulting wave velocities are shown in Fig. 3. Here, the wave velocity $w$ was expressed on a coordinate of dimensionless distance $z^*$ from the nozzle. It was defined as:

$$z^* = \frac{2gz}{V^2}, \tag{6}$$

where $g$ is the gravitational acceleration and $V$ a mean injection velocity. The falling velocity of the liquid column was predicted by a simple inviscid model. By using the Bernoulli's equation and the equation of continuity, the liquid column diameter $d(z^*)$ and the liquid velocity $v(z^*)$ were described as follows (Middleman, 1995):

$$d(z^*) = D(1+z^*)^{-1/4}, \tag{7}$$

$$v(z^*) = V(1+z^*)^{1/2}. \tag{8}$$

The solid line in Fig. 3 indicates the liquid velocity $v(z^*)$. It was shown that the wave velocity $w(z^*)$ was equivalent to the liquid velocity $v(z^*)$. It indicated that the surface wave was fixed on the liquid surface and was elongated with the elongation of the liquid column. It was also reasonable to assume the wave velocity as follows:

$$w(z^*) = V(1+z^*)^{1/2}. \tag{9}$$

### 3.2. Elongation of surface waves on a laminar liquid jet

Spectra of the surface wave motion were measured at various positions of the laminar liquid jet. Fig. 4 shows an example of the frequency spectra at various $z/L_b$, where $L_b$ was the breakup length of the jet. From these data, the spectrum intensity of the surface wave was mapped on the axial distance vs. frequency diagram. Fig. 5 shows the monotone intensity expression of the spectrum. The gray level indicates the height of spectrum components. Many discrete peaks appeared at the middle portion of the liquid column. Frequencies of these peaks were not in harmonic relationship with each other. This result indicated that the surface wave consisted of several wave components of various modes. Near the breakup point, the spectrum became broader. That is to say, the breakup phenomena included the irregular behavior even in a laminar liquid jet.

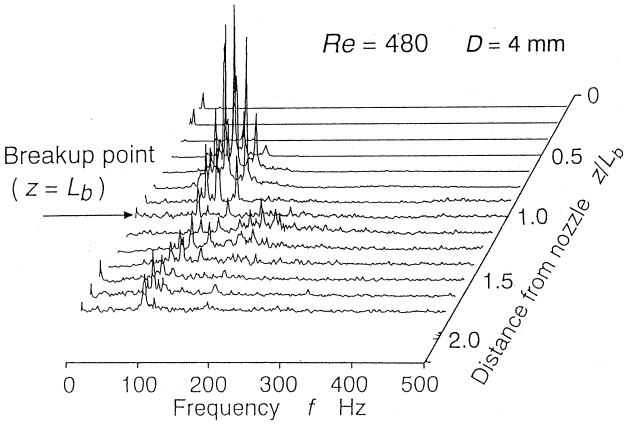


Fig. 4. Spectrum structure of surface waves on liquid column.

Here, we consider the small amplitude wave of wavelength $\lambda(z^*)$ appearing on a liquid column whose diameter is $d(z^*)$. Since the wave was elongated with an elongation of the liquid column as mentioned above, the liquid volume in unit wavelength, $\lambda(z^*) \times \pi d^2(z^*)/4$ was conserved. Therefore, we could obtain the following relation considering the equation of continuity:

$$\frac{\mathrm{d}}{\mathrm{d}z^*}\left[\lambda(z^*)\frac{\pi\{d(z^*)\}^2}{4}\right] = 0. \tag{10}$$

From this relation, if we assume that an initial wave $\lambda(z_0^*)$ appeared at $z^* = z_0^*$, its wavelength might change with the flow

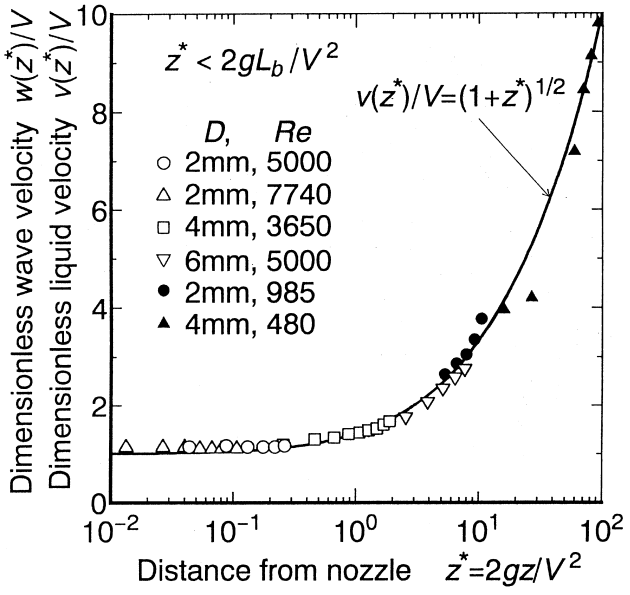


Fig. 3. Relation between wave velocity and liquid velocity.

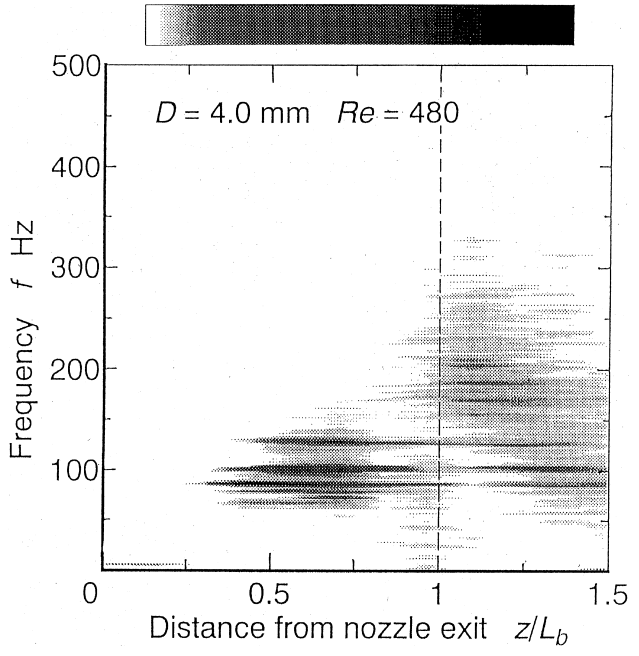


Fig. 5. Change of spectrum components along flow direction.

direction. The change of the wavelength is expressed by $\lambda(z_0^*|z^*)$ and this wavelength was derived from Eq. (10).

$$\lambda(z_0^*|z^*) = \lambda(z_0^*)\left\{\frac{(1+z^*)}{(1+z_0^*)}\right\}^{1/2}. \tag{11}$$

Eq. (11) indicates that the wavelength increased with an increase of $z^*$. Now, we consider the result of the Rayleigh's analysis to proceed with further discussions. Rayleigh's theory showed that the wavelength of the instability wave having the maximum growth rate was described as:

$$\lambda = 4.51d. \tag{12}$$

Thereby, we assume that the initial wave $\lambda(z_0^*)$ described in Eq. (11) is the Rayleigh wave. That is:

$$\lambda(z_0^*) = 4.51d(z_0^*) = 4.51D(1+z_0^*)^{-1/4}. \tag{13}$$

By substituting it into Eq. (11), we obtain the following equation:

$$\lambda(z_0^*|z^*) = \frac{4.51D}{(1+z_0^*)^{3/4}}(1+z^*)^{1/2}. \tag{14}$$

This equation indicates that the wave which had the origin in the Rayleigh wave at $z^* = z_0^*$ changed its wavelength through the development. Fig. 6 shows the elongation process of the Rayleigh wave appearing at $z_0^* = 0, 2, \ldots, 8$. In this figure, liquid column diameter calculated by Eq. (7) and the wavelength of the Rayleigh wave calculated by Eq. (13) are also shown.

By using Eqs. (4) and (9), the frequency diagram (Fig. 5) could convert to the wavelength diagram. Fig. 7 shows this converted result. Three large wave components were also shown in the diagram. Wavelengths of these waves were gradually increased with an increase of the distance from the nozzle. Solid line $\lambda(0|z^*)$ in the figure indicated the change of wavelength when the Rayleigh wave appeared at the nozzle exit. And the wavelength when the Rayleigh wave appeared at the breakup point was indicated by the symbol (•) in the figure. Wavelengths of the surface waves observed on the liquid column were shorter than that of the Rayleigh wave at the nozzle exit and longer than that of the Rayleigh wave at breakup point. Broken line indicates $\lambda(z_0^*)$ obtained by Eq. (13). It seemed that the surface wave of large amplitude appeared after

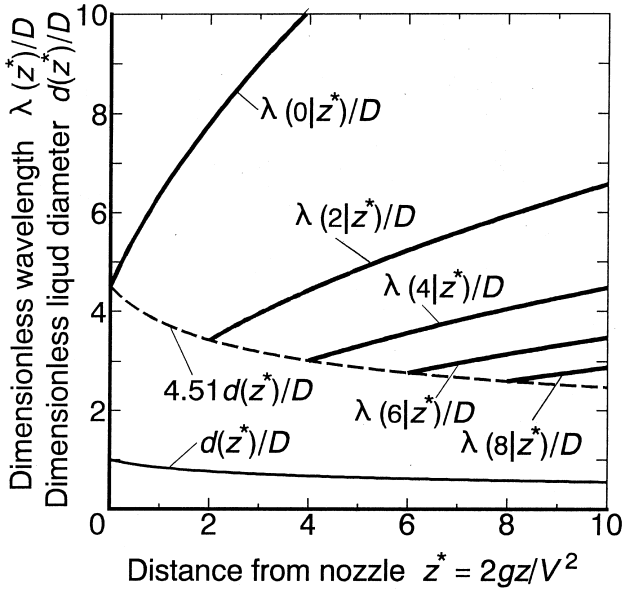


Fig. 6. Elongation of Rayleigh wave on liquid column.

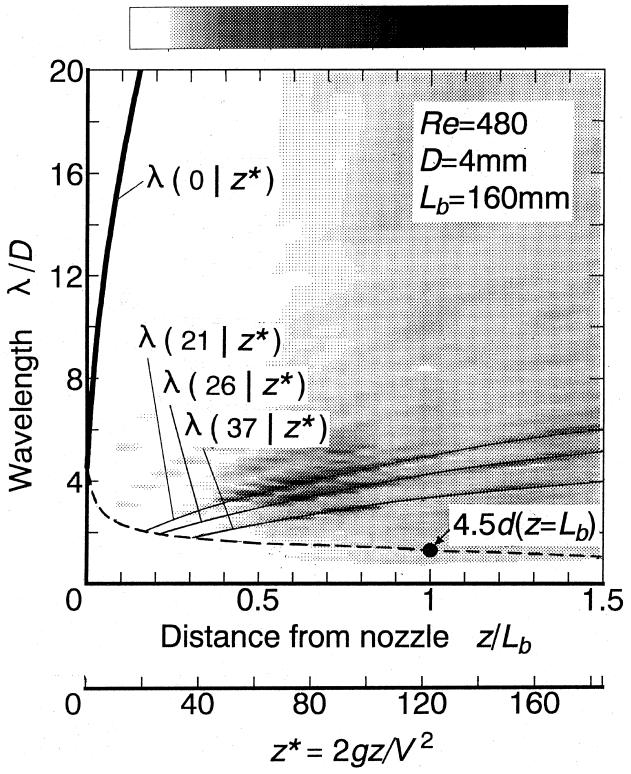


Fig. 7. Change of wavelength along flow direction.

it passed the location where its wavelength coincided with $\lambda(z_0^*)$ of the Rayleigh wave i.e. broken line. Further, we could find out $\lambda(21|z^*)$, $\lambda(26|z^*)$ and $\lambda(37|z^*)$ as the fitted wavelengths calculated by Eq. (14). It means that the elongation process of the surface wave is well described by this analysis.

### 3.3. Cross-correlation analysis for the wave structure

In order to discuss the spatial structure of the surface wave on a laminar liquid jet, the method of a cross-correlation analysis was used (Ohji and Amagai, 1988). Two sensors were named in sensor-1 and sensor-2 in the following part. The positions of these sensors were indicated as $z_1$ and $z_2$, respectively. Cross-correlation between two signals of these sensors was calculated by Eq. (3).

Overall cross-correlations were investigated at first to obtain the general behavior of wave development. Sensor-1 was fixed at the breakup point ($z_1 = 180$ mm) and the sensor-2 was traversed on the various positions on the liquid column. Fig. 8 shows the results. Data corresponding to $L_b = 180$ mm was the auto-correlation obtained from the sensor-1 signal. By this method, we could evaluate the similarity of the wave motions between breakup position and other positions. Cross-correlation function includes the phase information of the waves. If the signals between two sensors are similar and have the same phase, the cross-correlation becomes positive. On the other hand, if the two signals are similar but have the opposite phase, the cross-correlation has a negative value. Moreover, if two signals are completely different from each other, the cross-correlation becomes zero.

Now, we focus a discussion on the data at $z_2 = 180$ mm. In this case, the cross-correlation function became equivalent to the auto-correlation function. Periodical peaks were observed in the data, and the peak levels gradually reduced with an increase of $|\Delta t|$. This result indicated that the similar wave

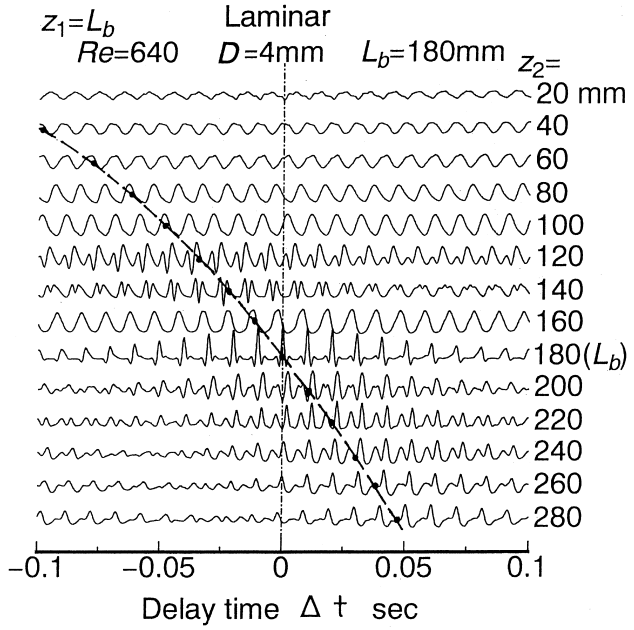


Fig. 8. Overall cross-correlation structure of surface wave.

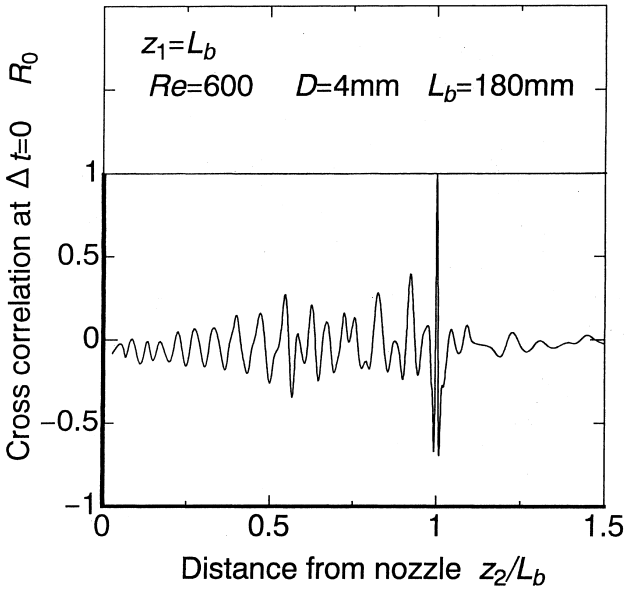


Fig. 9. Simultaneous cross-correlation of surface wave.

motions appeared periodically every time delay of $\Delta t \approx 0.01$ s. However, since the wave motions included the irregular components, the similarity between two wave motions during the long time delay became low. This result was agreed with the spectrum analysis, i.e., the spectrum included the broad band components near the breakup point.

Next, we pick up the case of $z_2 = 100$ mm to understand the meaning of the data in Fig. 8. This data reviewed the relationship between surface wave near the breakup point and the surface wave at $z_2 = 100$ mm. The value of cross-correlation changed periodically between positive and negative values against $\Delta t$. Therefore, we can conclude that the two surface waves observed at breakup position and $z_2 = 100$ mm included similar wave components. Time delay $\Delta t$ between peak to peak was 0.01 s at $z_2 = 100$ mm. This value was equivalent as the data at breakup point. It seemed that the sinusoidal wave appeared on the liquid column at $z_2 = 100$ mm which has a similar frequency with the breakup wave.

At the condition of $z_2 = 120$ mm, the wave pattern in the cross-correlation had double components. This wave pattern indicated that the two different waves were overlapped with each other. It supported that the surface wave consisted of some wave components with different wavelengths. These wave components showed the different frequency peaks in the spectrum diagram mentioned before.

A broken line in Fig. 8 indicates the passing time of one wave which might pass the breakup point at the time of $\Delta t = 0$. This line was derived from Eq. (9) as:

$$\Delta t_{\mathrm{p}}(z_2^*) = \frac{V}{g}\left\{\left(1+z_2^*\right)^{1/2} - \left(1+z_1^*\right)^{1/2}\right\}. \tag{15}$$

The number of peaks on the cross-correlation diagram between $\Delta t_{\mathrm{p}}(z_2^*)$ line and $\Delta t = 0$ at each $z_2$ shows the wave number on the column between $z_2$ and breakup point.

Simultaneous cross-correlation $R_0$ was derived as the function of $z_2$ where the sensor-1 was fixed at breakup point. Fig. 9 shows the result. This is equivalent to the variation of cross-correlation on the axis at $\Delta t = 0$ in Fig. 8. In this case, the simultaneous signals of two sensors were multiplied with each other. Therefore, if the cross-correlation was positive, the surface wave at $z_2$ and the surface wave at breakup point have the same phase. On the other hand, if the correlation became negative, two waves have the opposite phase. In Fig. 9, the correlation at $z_2/L_b < 0.6$ changed periodically between positive and negative. However, the non-periodical change of correlation pattern appeared at $0.6 < z_2/L_b < 1.0$. This result indicated that the surface wave was modulated by several waves which had different modes of wavelength as described in Fig. 7. Distance between peak to peak in the data of Fig. 9 indicates the wavelength of surface wave. In the upstream region at $z_2/L_b < 0.6$, the distance between peak to peak gradually increased with an increase of the distance from the nozzle. It indicated that the surface wave was elongated as a sinusoidal wave within the early stage of development.

From Fig. 8, we can also derive the information about the surface wave deformation. The maximum value in the cross-

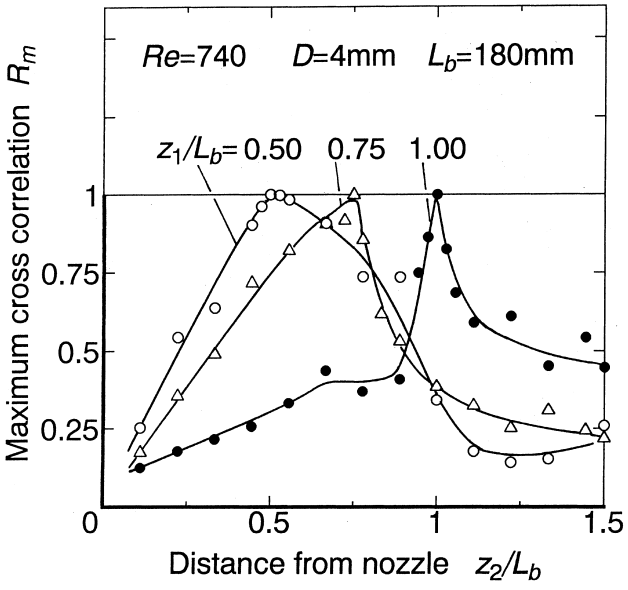


Fig. 10. Evaluation of wave deformations by cross-correlation.

correlation near the broken line was measured. These values indicated the similarity between wave motions at two different positions about one considering wave. Therefore, if the signals between two sensors were completely same, in other words, the wave pattern was completely conserved between the positions of two sensors, the correlation became unity. On the other hand, if the wave was deformed, the correlation became low. Therefore, we can obtained the information about the wave deformation from the analysis of the maximum cross-correlation $R_m$. Fig. 10 shows the result. Sensor-1 was fixed at $z_1/L_b = 0.5$, 0.75 and 1.0, and the sensor-2 was traversed on the liquid column. In the case of $z_1/L_b = 1.0$, the values of the maximum correlation became low when the distance between two sensors became large. At the case of $z_1/L_b = 0.5$ and 0.75, the maximum correlation kept the high values around the position of the sensor-1, however they became low when the sensor-2 approached the breakup point. These results indicated that the surface wave rapidly deformed when the wave came close to the breakup point.

## 4. Conclusions

By employing a new approach of frequency and cross-correlation analysis, the progress of surface wave and the breakup process of a laminar liquid jet from a round nozzle has been described. The important conclusions drawn from this work can be summarized as follows. Surface wave consisted of several wave components which have different wave modes. There was no relative velocity between liquid and wave, and the surface wave was elongated with an elongation of the liquid column by the effect of gravity. The wavelength of the surface wave actually appearing on the laminar liquid jet was shorter than the wavelength of Rayleigh's instability wave developed from the nozzle exit. The spatial structure and deformation behavior of the surface wave could be evaluated by the cross-correlation analysis. As a result, it was found that the surface wave rapidly deformed when the wave came close to the breakup point.

## Acknowledgements

This work was supported by the Grant-in-Aid of Scientific Research from the Ministry of Education (No.06750163). The experimental and technical supports by Mr. S. Akimoto, O. Onodera, K. Hayashida and G. Ogiwara in Gunma University are much appreciated.

## References

Amagai, K., Arai, M., 1997. Frequency analysis of disintegrating liquid column. In: Proceedings of the 7th International Conference on Liquid Atomization and Spray Systems, Seoul, South Korea, pp. 361–368.

Bogy, D.B., 1975. Droplet formation in a circular liquid jet. Ann. Rev. Fluid Mech. 11, 207–228.

Chaudhary, K.C., Redekopp, L.G., 1980. The nonlinear capillary instability of a liquid jet. Part 1. Theory. J. Fluid Mech. 96 (2), 257–274.

Donnelly, R.J., Glaberson, W., 1966. Experiments on the capillary instability of a liquid jet. Proc. Roy. Soc. Lond. A 290, 547–556.

Keller, J.B., Rubinow, S.I., Tu, Y.O., 1973. Spatial instability of a jet. Physics of Fluid 16 (12), 2052–2055.

Middleman, S., 1995. Modeling Axisymmetric Flows, Ch. 4. Academic Press, New York.

Ohji, M., Amagai, K., 1988. Structure of modulated wavy voltical flows in the circular Couette system. Fluid Dynamics Research 3 (1-4), 305–314.

Rayleigh, L., 1945. The Theory of Sound, vol. 2. Dover Publications, New York, p. 362.

Tanasawa, Y., Toyoda, S., 1955. On the atomization of liquid jet issuing from a cylindrical nozzle, Tech. Rep. Tohoku University 19, 135–156.

Tomotika, S., 1935. On the instability of a cylindrical thread of a viscous liquid surrounded by another viscous fluid. Proc. Roy. Soc. A 150, 322.